

Ir(III) Pincer Complex with Solo Coordinatively Active Site as a Surrogate for Half-Sandwich Catalysts: Enabling Asymmetric Acylnitrenoid Transfer and Structure–Activity Relationship Studies

Yun-Peng Chu,[†] Zhen-Hui Xu,[†] Jing Zhao, Chuanyong Wang, Constantin G. Daniliuc, and Jiajia Ma*Cite This: <https://doi.org/10.1021/jacs.5c12730>

Read Online

ACCESS |



Metrics & More

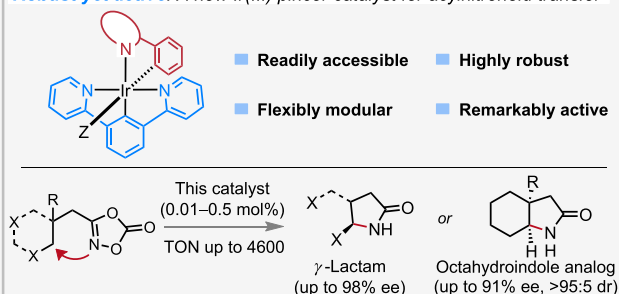


Article Recommendations



Supporting Information

ABSTRACT: Metal-acylnitrenoid-enabled asymmetric C(sp³)–H amidation has emerged as a highly effective synthetic strategy for accessing enantioenriched amides and chiral amines. While state-of-the-art transition metal catalysts typically feature a half-sandwich scaffold, the exploration of novel catalyst scaffolds remains intriguing. We herein introduce a new class of Ir(III) pincer complexes, which exhibit exceptional modularity and tunability in both steric and electronic properties. They have been demonstrated to function as highly efficient precatalysts (with loadings as low as 0.01 mol %) for C(sp³)–H amidation, enabling the synthesis of enantioenriched γ -lactams and octahydroindole derivatives. The remarkable robustness of these iridium complexes has been confirmed through treatments with strong acid and base, as well as heating and catalyst recovery experiments. Structure–activity relationship studies provided valuable insights into the underlying mechanisms driving the success of these Ir(III) complexes.

Robust yet active: A new Ir(III) pincer catalyst for acylnitrenoid transfer

INTRODUCTION

Direct asymmetric C(sp³)–H amination stands as one of the most ideal strategies for synthesizing nitrogen-containing molecules from readily available alkane feedstocks.^{1–3} Over the past decades, metal-nitrenoid mediated asymmetric C(sp³)–H amination has garnered significant attention due to its remarkable efficiency and selectivity.^{4–11} Early advancements showcased sulfamate-derived iminoiodinanes and sulfonyl azides as prominent nitrene precursors, which could be effectively harnessed by chiral metal-porphyrin,^{12–14} metal-salen,^{15,16} paddle-wheel dirhodium and diruthenium,^{17–21} metal-pybox,^{22,23} and chiral-only-at-metal complex,²⁴ among others.⁶ These studies predominantly yielded enantioenriched sulfamides, owing to the sulfonyl-derived nitrene precursors. Consequently, exploring alternative nitrene precursors has become a focal point, as it would lead to expanded product chemical space of chiral amines.

Recently, Chang and co-workers pioneered the use of dioxazolones as versatile acylnitrene precursors,^{25–27} enabling the synthesis of enantioenriched *N*-acylimides via asymmetric C(sp³)–H amidation (Figure 1a).^{28–31} This approach is particularly noteworthy not only for its atom-economical nature but also because the resulting *N*-acylimides are prevalent in drug molecules and can be readily diversified into various chiral amines and related derivatives. Notable contributions have also been made by Chen, He, and Wang,^{32–34} Yu,³⁵ Meggers and Houk,³⁶ Rovis,^{37–39} Yi and Zhou,⁴⁰ Matsunaga and Yoshino,⁴¹ Blakey and Baik,⁴² Li,^{43,44}

Xie, Yan, and Qi,⁴⁵ and others.^{46–50} The success of these endeavors is largely attributed to the tailored design of individual transition metal catalysts. For example, an interesting design by Meggers and co-workers is the octahedral chiral-at-metal complex.³⁶ However, it is noteworthy that the most widely adopted catalyst scaffold features a half-sandwich scaffold.^{51,52} These half-sandwich catalysts typically comprise a transition metal ion such as Ir(III), Ru(II), Os(II) etc., a pentamethylcyclopentadienyl anion (Cp[–]) or a *p*-cymene, a bidentate *N,O* or *N,N* ligand, and a labile monodentate ligand (Figure 1b).^{4,53–61} Despite this design has proven elegant and effective, there remains considerable interest to extend the chiral catalyst toolbox to a more expanded chemical space (Figure 1c). Inspired by all these great advancements and in line with our interest in both half-sandwich and octahedral transition metal complexes,^{62,63} we envisioned that the established half-sandwich complex could be redesigned into pincer counterpart, which is known for its remarkable thermodynamic stability. In light of the easy accessibility and widespread use of pyridine-benzene-pyridine (N[–]C[–]N[–]) and phenylpyridine or phenyloxazoline (C[–]N[–]) ligands in organo-

Received: July 25, 2025

Revised: September 25, 2025

Accepted: September 25, 2025

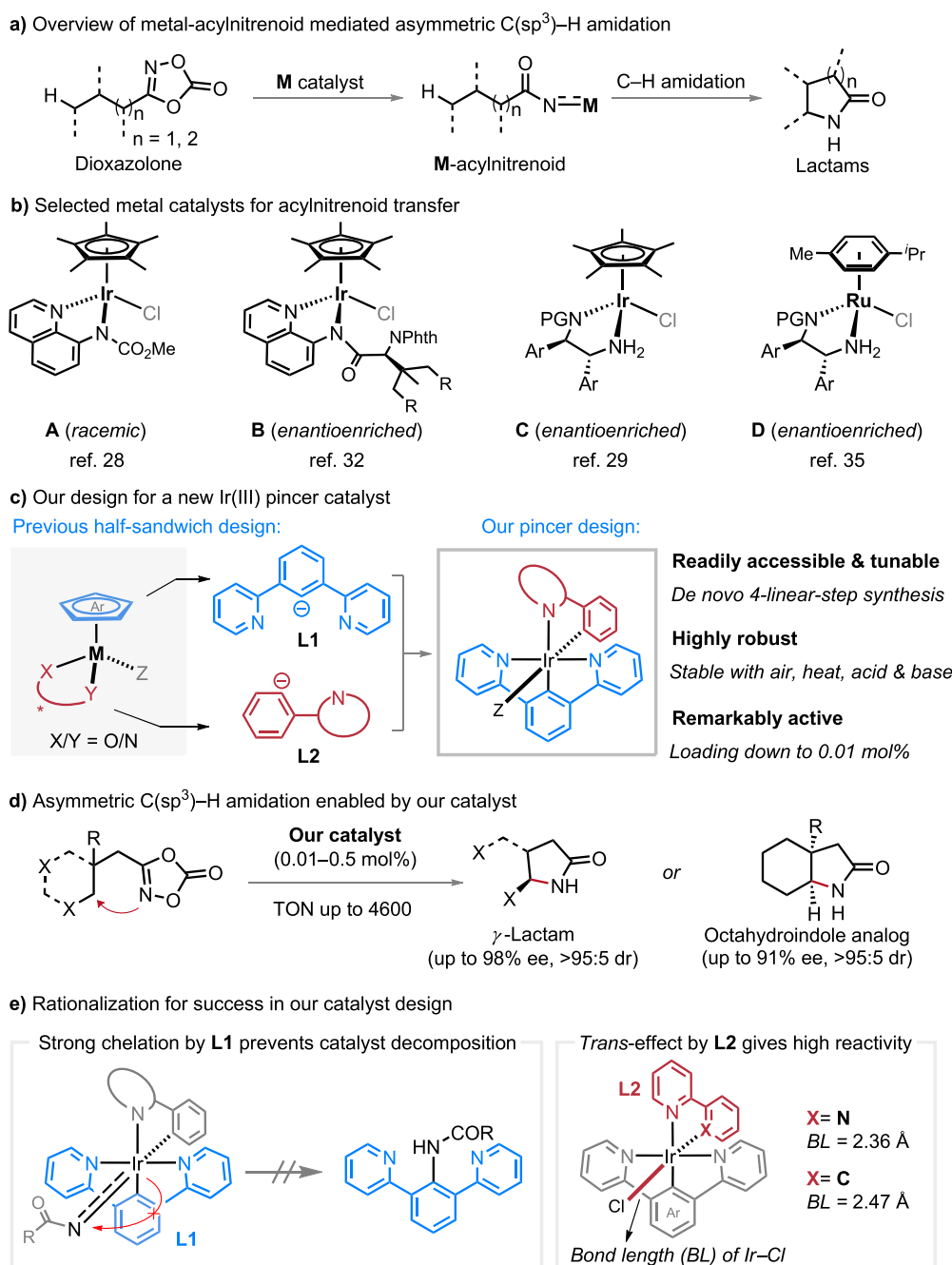


Figure 1. (a) Overview of metal-acylnitrenoid for asymmetric C(sp³)-H amidation; (b) Selected half-sandwich transition metal complexes for nitrene transfer; (c) Previous catalyst design vs our design for a new Ir(III) pincer catalyst; (d) Asymmetric C(sp³)-H amidation enabled by our catalyst; (e) Key factors for success in our catalyst design.

metallic chemistry, we hypothesized that a tridentate N[^]C[^]N ligand (**L1**) could serve as a surrogate for Cp*, while a bidentate C[^]N ligand (**L2**) could replace the N,O or N,N ligands. This design would result in an alternative transition metal pincer catalyst with solo coordinatively active site, thus acting as a surrogate for previous half-sandwich congeners.

We hereby report the realization of this concept through the development of the pincer [Ir(N[^]C[^]N)(C[^]N)(MeCN)]⁺ complex, which serves as an efficient catalyst scaffold for intramolecular asymmetric C(sp³)-H amidation through acylnitrene transfer. A variety of chiral phenyloxazolines (C[^]N ligands) can be employed to prepare these chiral iridium(III) complexes, thereby enabling the synthesis of

enantioenriched γ -lactams and octahydroindoles with high yields and excellent diastereo- and enantioselectivities (Figure 1d). Notably, the [Ir(N[^]C[^]N)(C[^]N)(MeCN)]⁺ complex exhibits several compelling features:

- 1) **Readily Accessibility and Tunability:** The Ir(III) complexes can be efficiently obtained through 4-linear-step synthesis. Moreover, they exhibit exceptional modularity, as they can be easily modified by leveraging the ever-expanding library of readily accessible tridentate N[^]C[^]N and bidentate C[^]N ligands. This versatility allows for precise tuning of the catalyst's electronic and steric properties by introducing electron-donating/withdrawing groups or using diverse enantiopure amino

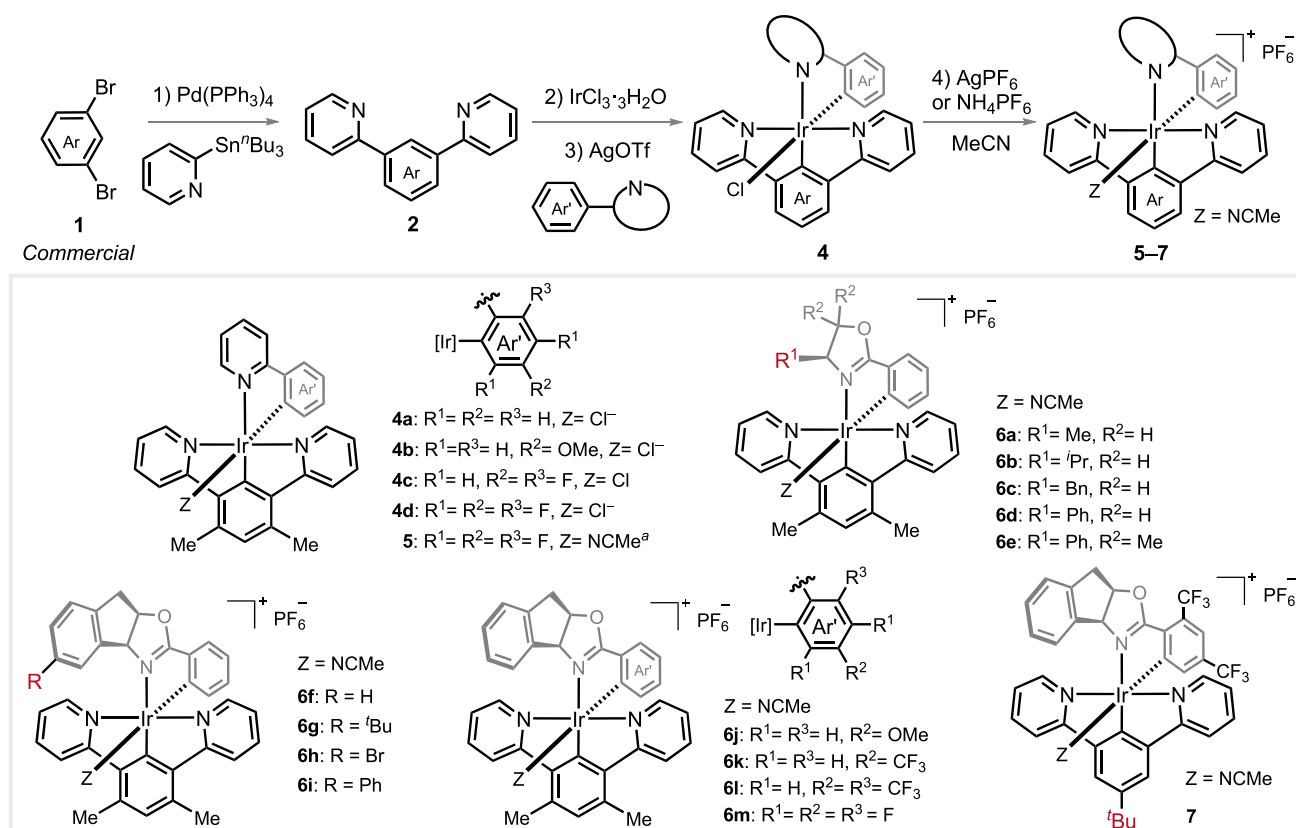
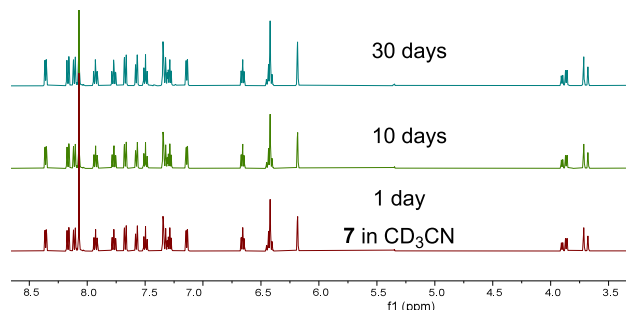
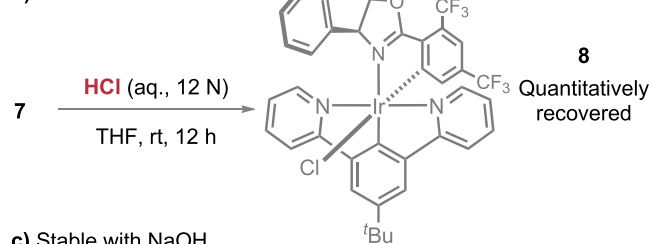


Figure 2. Ir(III) pincer complexes synthesis. ^aWith hexafluorophosphate as counterion. For more details, see SI.

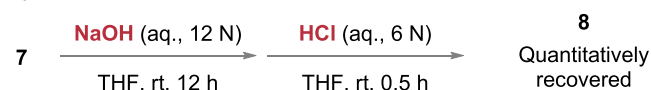
a) Stability investigation of 7 under ambient atmosphere



b) Stable with HCl



c) Stable with NaOH



d) Stable under heating

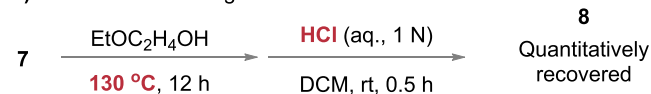


Figure 3. Stability investigation of 7. For more details, see SI.

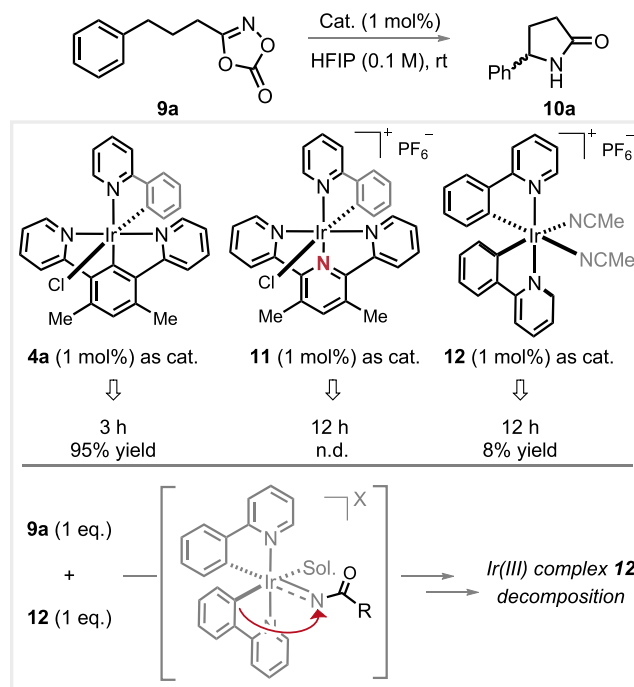


Figure 4. Catalytic performance of iridium complexes for intramolecular $\text{C}(\text{sp}^3)\text{-H}$ amidation and the tridentate $\text{N}^{\wedge}\text{C}^{\wedge}\text{N}$ ligand effect analysis. n.d. = not detected. For more details, see SI.

alcohols, thus enabling optimization for acylnitrenoid transfer.

2) High Robustness: The Ir(III) complex demonstrates remarkable stability under ambient conditions, remain-

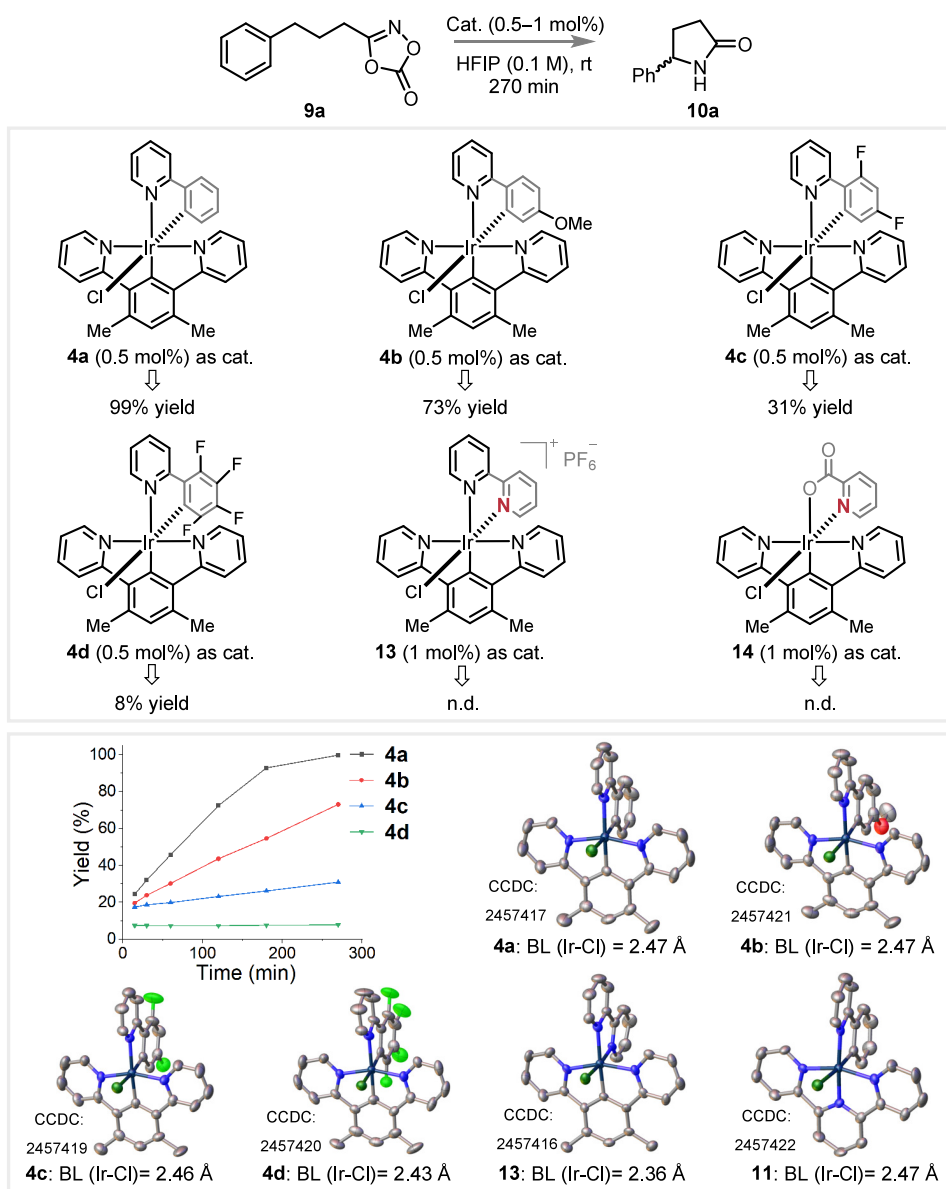


Figure 5. Investigation of the bidentate C^N ligand effect. X-ray crystallographic analysis shows longer Ir–Cl bond length in **4a** over **13**, which suggests remarkable *trans* effect by phenyl of cyclometalating bidentate C^N ligand. Longer Ir–Cl bond length in **4a** over **4c** and **4d** shows that the electron-withdrawing fluoro moieties weaken the *trans* effect while no influence was observed with the electron-donating methoxy (**4b**). n.d. = not detected. BL = bond length. For more details, see SI.

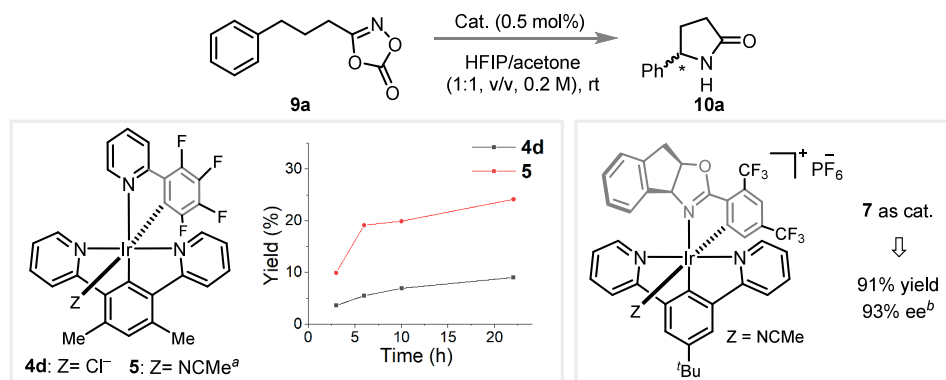


Figure 6. Probing the catalytic activity difference between the neutral (**4d**) and ionic (**5**) iridium complexes. Chiral iridium complex **7** has been identified as the optimal precatalyst for asymmetric C(sp³)–H amidation. ^aWith hexafluorophosphate as counterion. ^bTFE as solvent. For more details, see SI.

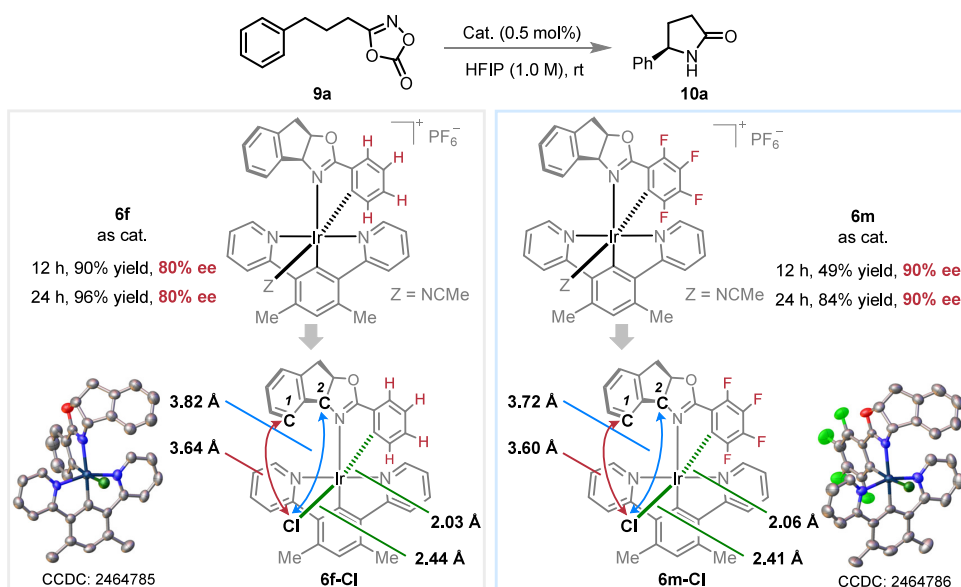


Figure 7. Probing the electron-withdrawing fluorine moieties effect on the catalysts' stereocontrol ability. X-ray crystallographic analysis shows shorter interatomic distance of Cl \rightarrow C1 and Cl \rightarrow C2 in **6m-Cl** over those in **6f-Cl**. This observation indicates that the indenyl of chiral cyclometalating C[^]N ligand in **6m** approaches closer to the coordinatively active site of catalyst, therefore providing enhanced stereocontrol for nitrene transfer.

ing intact in the presence of strong acid (HCl) or base (NaOH), as well as heating at 130 °C.

- 3) Remarkable Activity: The catalyst loading for C(sp³)-H amidation can be reduced to as low as 0.01 mol % (corresponding to 4600 TON), highlighting its high efficiency.

The success of this Ir(III) pincer catalyst can be attributed to two key factors:

- 1) Strong Chelation by the Pincer-Type N[^]C[^]N Ligand: The tridentate ligand N[^]C[^]N provides robust chelation,⁶⁴ which disfavors inner-sphere C-N coupling—a contrast to the behavior observed with bidentate C[^]N ligands in half-sandwich complexes, as reported by Chang.²⁸ The cooperation of tridentate N[^]C[^]N with cyclometalating bidentate C[^]N ligands leads to significantly enhanced thermodynamic stability of the entire Ir(III) complex.
- 2) Strong *Trans* Effect by the Cyclometalating C[^]N Ligand: The σ -donating ability of phenyl in C[^]N ligand leads to a strong *trans* effect on the labile chloride ion or MeCN ligands, thus facilitating rapid ligand exchange kinetics. This property is critical for achieving high catalytic activity.⁶⁵

RESULTS AND DISCUSSION

Synthesis of Iridium(III) Complexes. Inspired by Rovis' intriguing work on using a remarkable octahedral iridium(III) complex as photocatalyst,^{66–69} we commenced our study by synthesizing related analogues 4–7. As outlined in Figure 2, commercially available feedstocks dibromobenzene **1** and 2-(tributyltin)pyridine underwent Pd-catalyzed Stille cross-coupling to afford the N[^]C[^]N ligand **2**. Subsequently, heating a mixture of ligand **2** and IrCl₃·3H₂O in EtOCH₂CH₂OH/H₂O at 90 °C yielded the iridium dimer complex, which was used directly without further purification. To the obtained iridium dimer in EtOCH₂CH₂OH, the C[^]N ligand **3**

(phenylpyridine or enantioenriched phenyloxazoline) and AgOTf were added, and the resulting mixture was heated to 90–120 °C. The following column chromatography purification produced the target complex **4**. Alternatively, the labile ligand exchange between the Cl[−] anion and MeCN was conducted to provide complexes **5**–**7**. It is worth noting that some phenylpyridines (C[^]N ligand **3**) are commercially available, while most phenyloxazolines (C[^]N ligand **3**) can be obtained by a single-step condensation from commercial aldehydes and enantioenriched 1,2-amino alcohols.

Stability Investigation. Next, we evaluated the thermodynamic stability of the obtained complex. Complex **7** demonstrated exceptional stability, remaining intact for more than 30 days in CD₃CN under ambient conditions, as confirmed by ¹H NMR analysis (Figure 3a). Further, complex **7** could be quantitatively recovered as a chloride anion binding neutral complex **8** after treatment with either HCl (aqueous 12 N), NaOH (aqueous 12 N) or heated at 130 °C in EtOCH₂CH₂OH (Figure 3b–d). These findings collectively underscore the high robustness of complex **7**, making it a promising candidate for practical applications in challenging catalytic environments.

Catalytic Performance Investigation and Tridentate N[^]C[^]N Ligand Effect Analysis. To evaluate the catalytic activity of the synthesized iridium(III) complexes, dioxazoline **9a** and iridium complex **4a** (1 mol %) were combined in HFIP and stirred at room temperature for 3 h (Figure 4). Remarkably, complete conversion of **9a** was achieved, and the desired C(sp³)-H amidation product **10a** was isolated in an excellent yield of 95%, validating the efficacy of our catalyst design. In contrast, iridium(III) complex **11**, featuring a terpyridyl ligand, and complex **12**, with two bidentate cyclometalating phenylpyridine ligands, exhibited significantly reduced catalytic activity. Notably, when complex **12** was treated with **9a** (1 equiv) in HFIP, the iridium complex underwent remarkable decomposition. This decomposition was attributed to an inner sphere C-N coupling between the

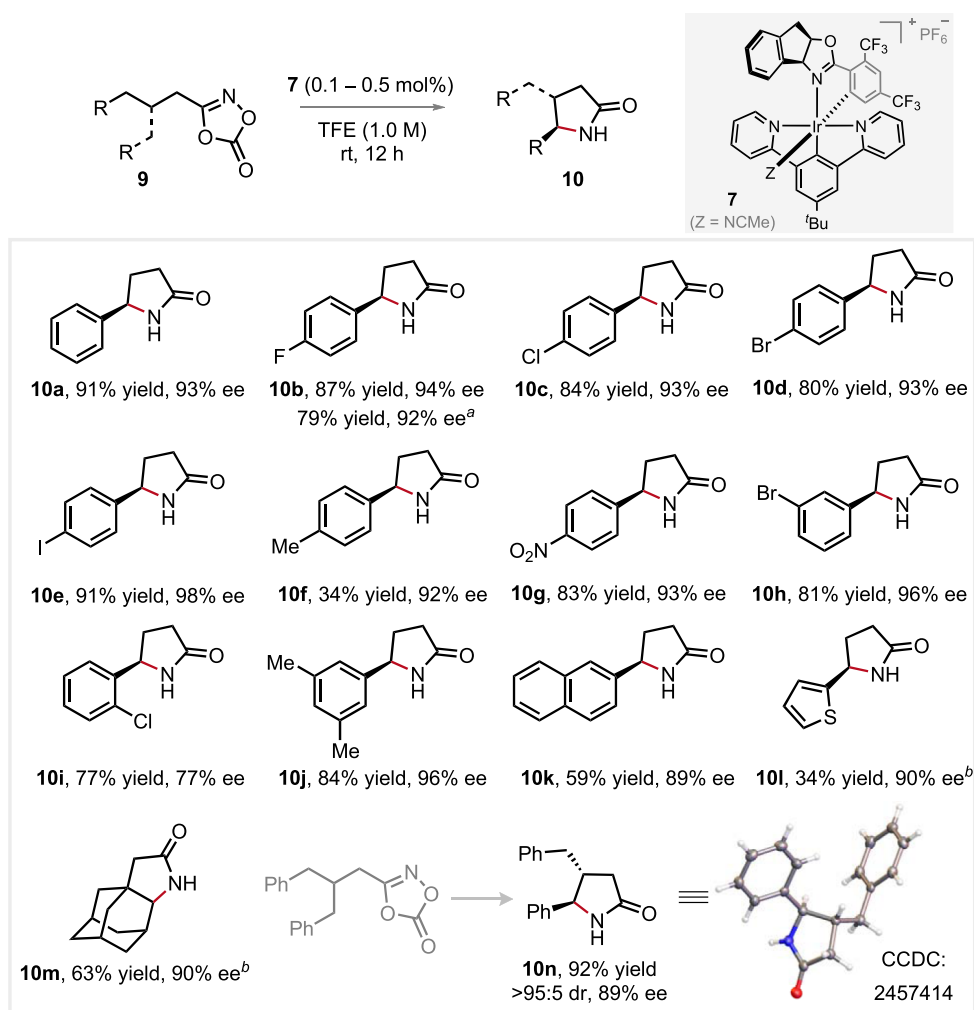


Figure 8. Scope of enantioenriched γ -lactams. Conditions: **9** (0.2 mmol) and **7** (0.5 mol %, 0.001 mmol) in TFE (1.0 M, 0.2 mL) were stirred at room temperature for 12 h under air. ^a0.1 mol % of **7** was used with a prolonged reaction time of 24 h and heated at 50 °C. ^bReaction was performed for 24 h.

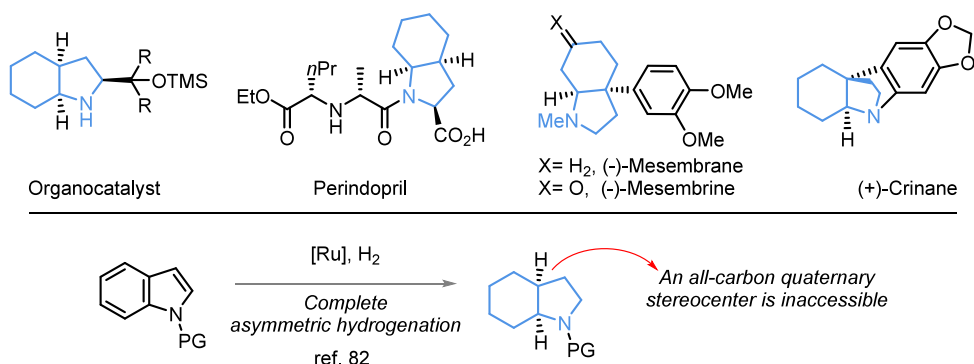


Figure 9. Octahydroindoles are significant scaffolds among organocatalyst and drug.

bidentate cyclometalating phenylpyridine ligand and the Ir-nitrenoid moiety, a pathway previously independently reported by Chang²⁸ and Yi and Zhou.⁷⁰ Interestingly, iridium complex decomposition was not observed when a tridentate $\text{N}^{\wedge}\text{C}^{\wedge}\text{N}$ ligand was employed. These findings collectively highlight that while bis-cyclometalating ligands are crucial for leveraging the catalytic activity of iridium(III) complexes, the strong chelation provided by the tridentate $\text{N}^{\wedge}\text{C}^{\wedge}\text{N}$ ligand is indispensable for maintaining thermodynamic stability.

Bidentate $\text{C}^{\wedge}\text{N}$ Ligand Effect Analysis. To investigate the influence of bidentate $\text{C}^{\wedge}\text{N}$ ligands, electron-donating methoxy (**4b**) and electron-withdrawing fluoro moieties (**4c** and **4d**) were introduced to the phenyl ring of the $\text{C}^{\wedge}\text{N}$ ligand. The catalytic activities of the resulting iridium(III) complexes **4b–d** were found to be inferior to that of **4a**, as evidenced by GC yields and reaction profiles (Figure 5). Further X-ray crystallographic analysis of the single-crystal structures revealed that the Ir–Cl bond length in **4a** (2.47 Å) is remarkably longer

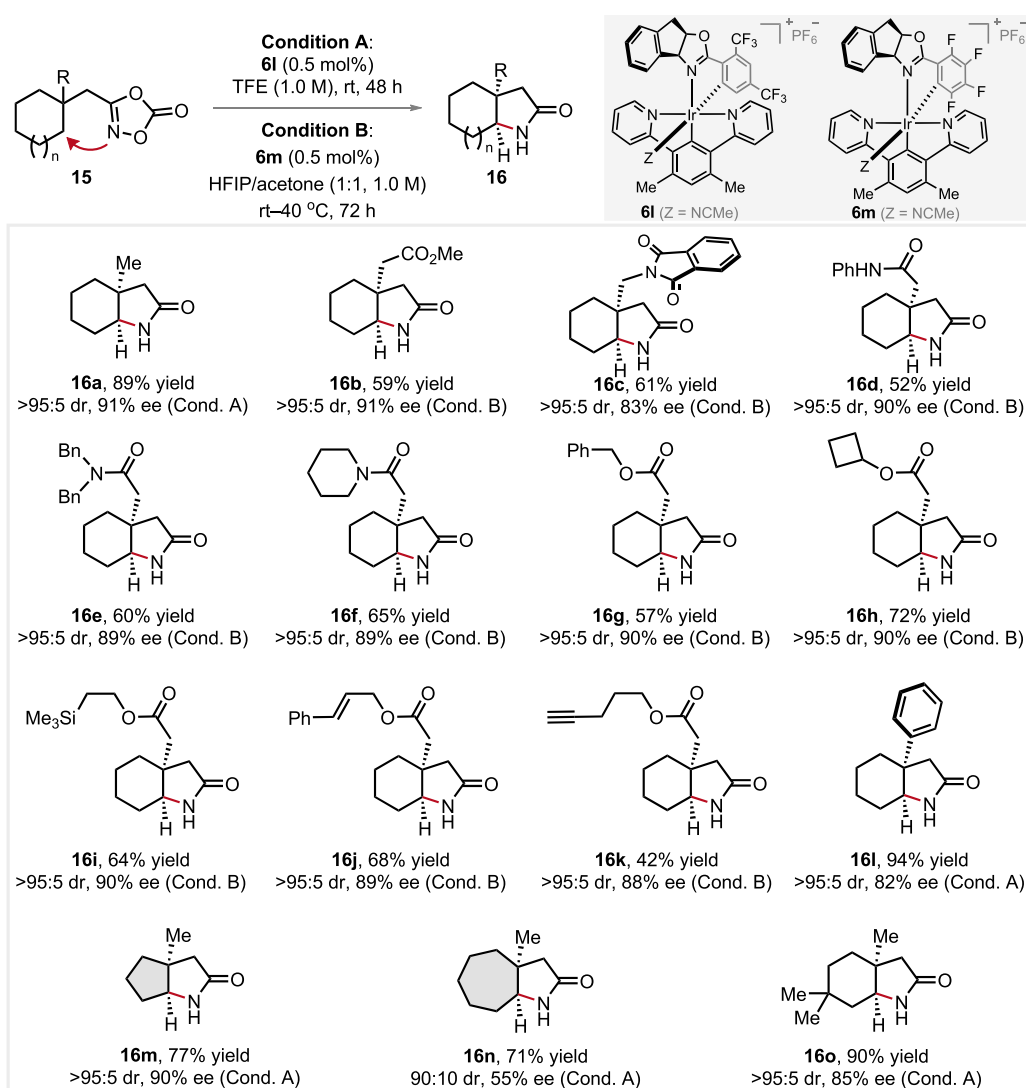


Figure 10. Scope of enantioenriched octahydroindole analogs.

than those in **4c** (2.46 Å)⁷¹ and **4d** (2.43 Å). Given that the *trans* effect is known to correlate with reaction rates,⁶⁵ the reduced catalytic activity of **4c** and **4d** can be attributed to the weakened *trans* effect caused by the decreased σ -donating ability of the di- and tetrafluoro-phenyl moieties. To further elucidate the role of the cyclometalating phenyl in maintaining the *trans* effect, a single crystal of complex **13**, featuring a bipyridine ligand, was analyzed. This complex exhibited a notably short Ir–Cl bond length of 2.36 Å. Likewise, complex **11**, with an Ir–Cl bond length of 2.47 Å, suggests that while the tridentate terpyridyl ligand results in the loss of catalytic activity, it does not influence the *trans* effect. Additionally, the failure of complexes **13** and **14**, which incorporate bipyridine and picolinate ligands, respectively, instead of phenylpyridine (**4a**), in catalyzing C(sp³)–H amidation, reaffirms that the bis-cyclometalating design is critical for success. In a short summary, these observations highlight that the *trans* effect induced by the phenyl of the bidentate C[^]N ligand is essential for achieving exceptional reaction efficiency.

Probing Activity Difference between the Neutral (4d**) and Ionic (**5**) Iridium Complexes.** While the neutral iridium complexes synthesized in this study exhibited good solubility in HFIP, solubility issues arose when using other solvents such as

acetone or THF. To address this, the neutral iridium complex **4d** was converted to its ionic counterpart **5**, incorporating hexafluorophosphate as the counterion. This modification significantly enhanced solubility in a broader range of solvents. As a result, a higher reaction rate was observed for **5** compared to **4d** when using a mixed solvent system of HFIP/acetone (1:1, v/v) (Figure 6). However, the difference in reaction rates was negligible in pure HFIP (see SI for details). Further screening of chiral iridium(III) complexes **6**–**7** identified **7** as the optimal precatalyst, achieving the synthesis of γ -lactam **10a** with an excellent enantiomeric excess of 93% (see SI for screening details).

Probing Stereocontrol Difference between **6f and Its Fluorinated Counterpart **6m**.** The chiral iridium(III) complexes incorporating electron-withdrawing substituents (F and CF₃) on the cyclometalating bidentate C[^]N ligand consistently demonstrated enhanced stereocontrol compared to their unsubstituted counterparts according to precatalyst screening experiments (see SI). For instance, the iridium(III) complex **6f** yielded product **10a** with an ee of 80%, while its tetra-fluorinated analog **6m** exhibited a significantly higher ee of 90% (Figure 7). To investigate the underlying mechanism, single-crystal X-ray diffraction analysis was conducted on their

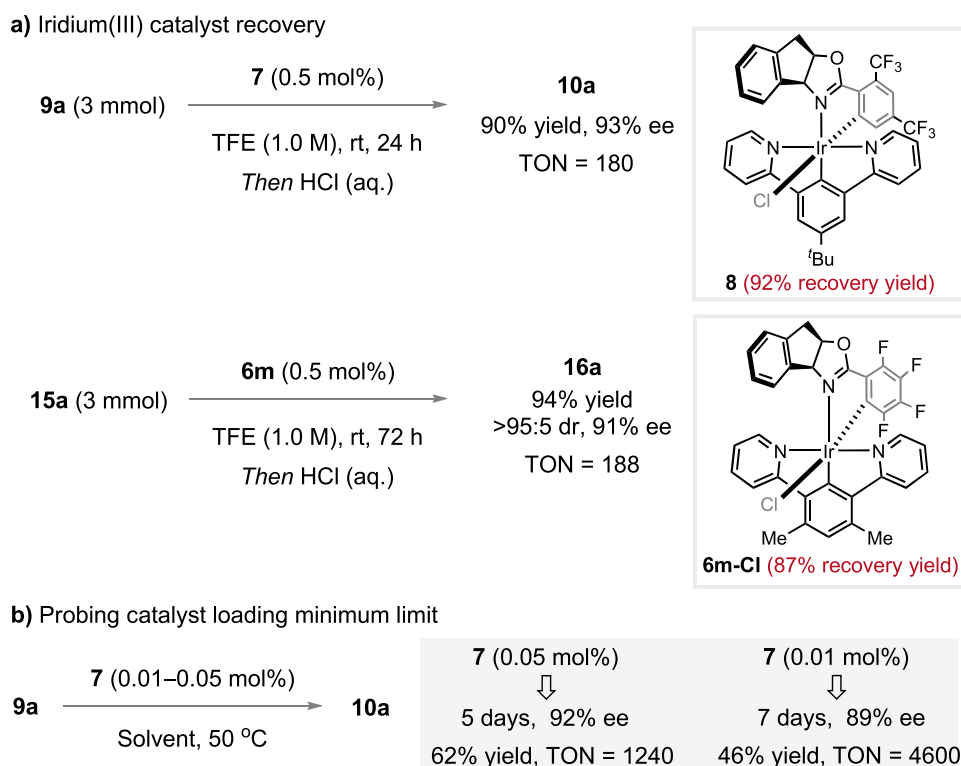


Figure 11. Catalyst recovery and probing catalyst loading minimum limit. For reaction details, see SI.

corresponding Cl-binding neutral congeners, **6f-Cl** and **6m-Cl**. As illustrated in Figure 7, the distances between Cl and C1 (Cl→C1) as well as Cl and C2 (Cl→C2) in **6m-Cl** were measured at 3.60 Å and 3.72 Å, respectively, whereas those in **6f-Cl** were 3.64 Å and 3.82 Å. This observation clearly indicates that the indenyl moiety of the chiral C^{^N} ligand approaches the coordinatively active site (occupied by the Cl anion) more closely upon the introduction of four fluorine substituents. Consequently, the tetra-fluorinated complex **6m** exhibits superior stereocontrol in the nitrene transfer reaction.

The observed variation in the distance between the Cl anion and the indenyl moiety from **6f-Cl** to **6m-Cl** can be attributed to both the elongation of the equatorial Ir–C bond (2.03 Å to 2.06 Å) and the shortening of the Ir–Cl bond (2.44 Å to 2.41 Å). These phenomena can be rationalized as follows: first, the introduction of electron-withdrawing fluoro substituents to the phenyl ring of the cyclometalating C^{^N} ligand reduces its σ -donating ability, resulting in an elongated Ir–C bond (2.03 Å to 2.06 Å). Simultaneously, the chiral C^{^N} ligand remains tightly chelated to the metal center, causing the distal indenyl moiety to move closer to the Cl ion. This movement can be analogously described as resembling the action of a pump jack. Second, the diminished σ -donating ability due to the fluorine substituents weakens the *trans* effect, leading to a shortened Ir–Cl bond (2.44 Å to 2.41 Å). Consequently, the Cl ion (representing the coordinatively active site) moves closer to both the metal center and the indenyl moiety of the C^{^N} ligand. Collectively, these findings provide a plausible explanation for the enhanced stereocontrol achieved through the incorporation of electron-withdrawing groups on the chiral C^{^N} ligand.

Generality and Scope Evaluation. Having established the optimal conditions for intramolecular C(sp³)–H amidation, we proceeded to evaluate the scope of γ -lactam synthesis.

As illustrated in Figure 8, a range of functional groups, including halogens (fluorine, chloro, bromo, iodine) and methyl groups, were well tolerated, yielding products (**10b–10f**, **10h–10j**) with up to 91% yield and 98% ee, while the ortho substituent Cl gives moderate ee of 77% (**10i**). A strong electron-withdrawing nitro group did not negatively impact the reaction outcome (**10g**). Moreover, thiophene or naphthyl moieties (**10k–10l**) also delivered satisfactory yields and good ee. The asymmetric C(sp³)–H amidation was successfully applied to an adamantanyl ring, affording **10m** with 90% ee. Additionally, a β,γ -disubstituted lactam **10n** was obtained as a single diastereomer with 89% ee through desymmetric C(sp³)–H amidation. The relative and absolute configurations of **10n** were unambiguously determined by X-ray crystallographic analysis.

Octahydroindole and its derivatives are important structural motifs in organocatalysts, small-molecule drugs, and natural products (Figure 9).^{72,73} Despite significant synthetic efforts,^{74–81} catalytic asymmetric approaches for their preparation via C(sp³)–H amination with high diastereo- and enantioselectivities remain rare.^{29,32} A notable exception is the elegant indole hydrogenation protocol developed by Glorius and co-workers, which, however, is not applicable to octahydroindoles featuring quaternary bridgehead carbons.⁸² Chang's earlier work reported only one example of such an octahydroindole framework bearing an all-carbon quaternary center, but achieving moderate enantioselectivity.²⁹ Building on the success of γ -lactam synthesis, we subjected dioxazolone **15a** with a cyclohexyl ring to iridium(III)-catalyzed intramolecular C(sp³)–H amidation (Figure 10). After optimization (see SI for details), the target octahydro-2H-indol-2-one **16a** was obtained as a single diastereomer and with 91% ee. This desymmetric synthetic strategy readily enables the formation of an all-carbon quaternary stereocenter. This

protocol demonstrated broad functional group tolerance, including esters (**16b**, **16g–h**), phthalimide (**16c**), amides (**16d–f**), silane (**16i**), alkene (**16j**), and alkyne (**16k**). An aryl substituent was also compatible, affording **16l** with 82% ee. Notably, a five-membered ring (**16m**) underwent desymmetric C(sp³)–H amidation with excellent diastereo- and enantioselectivity, while a seven-membered ring (**16n**) resulted in moderate stereoselectivity. Enantioenriched octahydro-2*H*-indol-2-one **16o**, featuring a second quaternary carbon on the backbone, was also synthesized with good stereoselectivity. The absolute configuration of product **16a** was determined using single-crystal data obtained from its tosylation product **18** (see SI), while the configuration of products **16b–o** was assigned by analogy. Nonetheless, the facile variation of the octahydroindole backbone in this work demonstrates its remarkable complementation to the indole hydrogenation protocol.⁸²

Catalyst Recovery and Probing Catalyst Loading Minimum Limit. Capitalizing on the remarkable robustness of the iridium(III) complexes, we subsequently conducted catalyst recovery experiments. As depicted in Figure 11a, the chiral iridium(III) complexes **7** and **6m** were successfully recovered as their chloride-binding neutral counterparts **8** and **6m-Cl**, respectively, from the catalytic reaction mixtures following treatment with aqueous HCl solution. Furthermore, the catalyst loading could be minimized to 0.01 mol %, achieving good ee of 89% and yield of 46%, corresponding to a turnover number (TON) of 4600. Finally, synthetic transformations of the obtained octahydro-2*H*-indol-2-one **16a** were conducted to give derivatives **17–20** with maintained ee and as single diastereomers (see SI).

CONCLUSIONS

We have developed a new class of Ir(III) pincer complexes in which the steric and electronic properties can be readily tuned due to their remarkable modularity. Despite their high thermodynamic stability, these complexes exhibit significant catalytic activity for C(sp³)–H amidation via nitrene transfer. Asymmetric transformations were successfully achieved using the corresponding chiral iridium complexes, which can be efficiently recovered from the reaction mixture. Structure–activity relationship studies revealed two key factors contributing to the success of these Ir(III) complexes: strong chelation of the tridentate N[^]C[^]N ligand leverages the stability and *trans* effect induced by the bidentate cyclometalating ligand provides high reaction efficiency. This study emphasizes the critical role of transition metal complex design in balancing catalytic efficiency and stability, providing valuable insights for the development of robust, high performance transition-metal-based catalysts. Ongoing research in our laboratory is focused on expanding the synthetic applications of these Ir(III) catalysts, particularly in the realm of asymmetric hydrogenation.

ASSOCIATED CONTENT

Supporting Information

The Supporting Information is available free of charge at <https://pubs.acs.org/doi/10.1021/jacs.5c12730>.

Experimental procedures and analytical data for all new compounds(PDF)

Accession Codes

Deposition Numbers 2457414–2457417, 2457419–2457422, and 2464785–2464786 contain the supplementary crystallographic data for this paper. These data can be obtained free of charge via the joint Cambridge Crystallographic Data Centre (CCDC) and Fachinformationszentrum Karlsruhe Access Structures service.

AUTHOR INFORMATION

Corresponding Author

Jiajia Ma – Frontiers Science Center for Transformative Molecules, National Key Laboratory of Innovative Immunotherapy, Shanghai Key Laboratory for Molecular Engineering of Chiral Drugs, School of Chemistry and Chemical Engineering, Shanghai Jiao Tong University, Shanghai 200240, P. R. China; orcid.org/0000-0002-4339-0462; Email: majj@sytu.edu.cn

Authors

Yun-Peng Chu – Frontiers Science Center for Transformative Molecules, National Key Laboratory of Innovative Immunotherapy, Shanghai Key Laboratory for Molecular Engineering of Chiral Drugs, School of Chemistry and Chemical Engineering, Shanghai Jiao Tong University, Shanghai 200240, P. R. China

Zhen-Hui Xu – Frontiers Science Center for Transformative Molecules, National Key Laboratory of Innovative Immunotherapy, Shanghai Key Laboratory for Molecular Engineering of Chiral Drugs, School of Chemistry and Chemical Engineering, Shanghai Jiao Tong University, Shanghai 200240, P. R. China

Jing Zhao – College of Chemistry and Chemical Engineering, Yangzhou University, Yangzhou 225002, China

Chuanyong Wang – College of Chemistry and Chemical Engineering, Yangzhou University, Yangzhou 225002, China; orcid.org/0000-0001-9576-8589

Constantin G. Daniliuc – Organisch-Chemisches Institut, Universität Münster, Münster 48149, Germany; orcid.org/0000-0002-6709-3673

Complete contact information is available at: <https://pubs.acs.org/10.1021/jacs.5c12730>

Author Contributions

[†]Y.P.C. and Z.H.X. contributed equally.

Notes

The authors declare no competing financial interest.

ACKNOWLEDGMENTS

National Key R&D Program of China (2023YFA1508900), Natural Science Foundation of Shanghai (23ZR1432000), Shanghai Rising-Star Program (24QA2704100), Fundamental Research Funds for the Central Universities (25X010202131), National Natural Science Foundation of China (22201174), and Shanghai Jiao Tong University 2030 Initiative are gratefully acknowledged for financial support.

REFERENCES

- (1) Park, Y.; Kim, Y.; Chang, S. Transition Metal-Catalyzed C–H Amination: Scope, Mechanism, and Applications. *Chem. Rev.* **2017**, *117* (13), 9247–9301.
- (2) Collet, F.; Lescot, C.; Dauban, P. Catalytic C–H Amination: the Stereoselectivity Issue. *Chem. Soc. Rev.* **2011**, *40* (4), 1926–1936.

- (3) Xiong, T.; Zhang, Q. New Amination Strategies Based on Nitrogen-Centered Radical Chemistry. *Chem. Soc. Rev.* **2016**, *45* (11), 3069–3087.
- (4) Hong, S. Y.; Hwang, Y.; Lee, M.; Chang, S. Mechanism-Guided Development of Transition-Metal-Catalyzed C–N Bond-Forming Reactions Using Dioxazolones as the Versatile Amidating Source. *Acc. Chem. Res.* **2021**, *54* (11), 2683–2700.
- (5) Hayashi, H.; Uchida, T. Nitrene Transfer Reactions for Asymmetric C–H Amination: Recent Development. *Eur. J. Org. Chem.* **2020**, *2020* (8), 909–916.
- (6) Ju, M.; Schomaker, J. M. Nitrene Transfer Catalysts for Enantioselective C–N Bond Formation. *Nat. Rev. Chem.* **2021**, *5* (8), 580–594.
- (7) Du, B.; Chan, C. M.; Au, C. M.; Yu, W. Y. Transition Metal-Catalyzed Regioselective Direct C–H Amidation: Interplay between Inner- and Outer-Sphere Pathways for Nitrene Cross-Coupling Reactions. *Acc. Chem. Res.* **2022**, *55* (15), 2123–2137.
- (8) Kaur, R.; Jain, N. R.; Rh- and Ir-Catalyzed Enantioselective sp^3 C–H Functionalization. *Chem. Asian J.* **2022**, *17* (24), No. e202200944.
- (9) Li, H.-H.; Chen, X.; Kramer, S. Recent Developments for Intermolecular Enantioselective Amination of Non-Acidic C (sp^3)-H Bonds. *Chem. Sci.* **2023**, *14* (46), 13278–13289.
- (10) Ye, C.-X.; Meggers, E. Chiral-at-Ruthenium Catalysts for Nitrene-Mediated Asymmetric C–H Functionalizations. *Acc. Chem. Res.* **2023**, *56* (9), 1128–1141.
- (11) Luo, Y.; Zhang, X.; Xia, Y. Recent Advances in Transition-Metal Catalyzed Nitrene Transfer Reactions with Carbamates. *Chin. Chem. Lett.* **2024**, *35* (3), 108778.
- (12) Lang, K.; Torker, S.; Wojtas, L.; Zhang, X. P. Asymmetric Induction and Enantiodivergence in Catalytic Radical C–H Amination via Enantiodifferentiative H-Atom Abstraction and Stereoretentive Radical Substitution. *J. Am. Chem. Soc.* **2019**, *141* (31), 12388–12396.
- (13) Zhou, X.-G.; Yu, X.-Q.; Huang, J.-S.; Che, C.-M. Asymmetric Amidation of Saturated C–H Bonds Catalysed by Chiral Ruthenium and Manganese Porphyrins. *Chem. Commun.* **1999**, No. 23, 2377–2378.
- (14) Dydio, P.; Key, H. M.; Hayashi, H.; Clark, D. S.; Hartwig, J. F. Chemoselective, Enzymatic C–H Bond Amination Catalyzed by a Cytochrome P450 Containing an Ir(Me)-PIX Cofactor. *J. Am. Chem. Soc.* **2017**, *139* (5), 1750–1753.
- (15) Ichinose, M.; Suematsu, H.; Yasutomi, Y.; Nishioka, Y.; Uchida, T.; Katsuki, T. Enantioselective Intramolecular Benzylic C–H Bond Amination: Efficient Synthesis of Optically Active Benzosultams. *Angew. Chem., Int. Ed.* **2011**, *50* (42), 9884–9887.
- (16) Nishioka, Y.; Uchida, T.; Katsuki, T. Enantio- and Regioselective Intermolecular Benzylic and Allylic C–H Bond Amination. *Angew. Chem., Int. Ed.* **2013**, *52* (6), 1739–1742.
- (17) Reddy, R. P.; Davies, H. M. L. Dirhodium Tetracarboxylates Derived from Adamantylglycine as Chiral Catalysts for Enantioselective C–H Aminations. *Org. Lett.* **2006**, *8* (22), 5013–5016.
- (18) Nasrallah, A.; Boquet, V.; Hecker, A.; Retailleau, P.; Darses, B.; Dauban, P. Catalytic Enantioselective Intermolecular Benzylic C(sp^3)-H Amination. *Angew. Chem., Int. Ed.* **2019**, *58* (24), 8192–8196.
- (19) Zalatan, D. N.; Du Bois, J. A Chiral Rhodium Carboxamidate Catalyst for Enantioselective C–H Amination. *J. Am. Chem. Soc.* **2008**, *130* (29), 9220–9221.
- (20) Höke, T.; Herdtweck, E.; Bach, T. Hydrogen-Bond Mediated Regio- and Enantioselectivity in a C–H Amination Reaction Catalysed by a Supramolecular Rh(II) Complex. *Chem. Commun.* **2013**, *49* (73), 8009–8011.
- (21) Miyazawa, T.; Suzuki, T.; Kumagai, Y.; Takizawa, K.; Kikuchi, T.; Kato, S.; Onoda, A.; Hayashi, T.; Kamei, Y.; Kamiyama, F.; Anada, M.; Kojima, M.; Yoshino, T.; Matsunaga, S. Chiral Paddle-Wheel Diruthenium Complexes for Asymmetric Catalysis. *Nat. Catal.* **2020**, *3* (10), 851–858.
- (22) Milczek, E.; Boudet, N.; Blakey, S. Enantioselective C–H Amination Using Cationic Ruthenium(II)-pybox Catalysts. *Angew. Chem., Int. Ed.* **2008**, *47* (36), 6825–6828.
- (23) Ju, M.; Zerull, E. E.; Roberts, J. M.; Huang, M.; Guzei, I. A.; Schomaker, J. M. Silver-Catalyzed Enantioselective Propargylic C–H Bond Amination through Rational Ligand Design. *J. Am. Chem. Soc.* **2020**, *142* (30), 12930–12936.
- (24) Zhou, Z.; Tan, Y.; Yamahira, T.; Ivlev, S.; Xie, X.; Riedel, R.; Hemming, M.; Kimura, M.; Meggers, E. Enantioselective Ring-Closing C–H Amination of Urea Derivatives. *Chem.* **2020**, *6* (8), 2024–2034.
- (25) Sauer, J.; Mayer, K. K. Thermolyse und Photolyse von 3-Substituierten Δ^2 -1,4,2-Dioxazolinonen-(5), Δ^2 -1,4,2-Dioxazolin-Thionen-(5) und 4-Substituierten Δ^3 -1,2,5,3-Thiadioxazolin-s-oxiden. *Tetrahedron Lett.* **1968**, *9* (3), 319–324.
- (26) Bizet, V.; Buglioni, L.; Bolm, C. Light-Induced Ruthenium-Catalyzed Nitrene Transfer Reactions: A Photochemical Approach towards N-Acyl Sulfinimides and Sulfoximines. *Angew. Chem., Int. Ed.* **2014**, *53* (22), 5639–5642.
- (27) van Vliet, K. M.; de Bruin, B. Dioxazolones: Stable Substrates for the Catalytic Transfer of Acyl Nitrenes. *ACS Catal.* **2020**, *10* (8), 4751–4769.
- (28) Hong, S. Y.; Park, Y.; Hwang, Y.; Kim, Y. B.; Baik, M.-H.; Chang, S. Selective Formation of γ -Lactams via C–H Amidation Enabled by Tailored Iridium Catalysts. *Science* **2018**, *359* (6379), 1016–1021.
- (29) Park, Y.; Chang, S. Asymmetric Formation of γ -Lactams via C–H Amidation Enabled by Chiral Hydrogen-Bond-Donor Catalysts. *Nat. Catal.* **2019**, *2* (3), 219–227.
- (30) Jung, H.; Kweon, J.; Suh, J.-M.; Lim, M. H.; Kim, D.; Chang, S. Mechanistic Snapshots of Rhodium-Catalyzed Acylnitrene Transfer Reactions. *Science* **2023**, *381* (6657), 525–532.
- (31) Jeong, J.; Jung, H.; Kim, D.; Chang, S. Multidimensional Screening Accelerates the Discovery of Rhodium Catalyst Systems for Selective Intra- and Intermolecular C–H Amidations. *ACS Catal.* **2022**, *12* (13), 8127–8138.
- (32) Wang, H.; Park, Y.; Bai, Z.; Chang, S.; He, G.; Chen, G. Iridium-Catalyzed Enantioselective C(sp^3)-H Amidation Controlled by Attractive Noncovalent Interactions. *J. Am. Chem. Soc.* **2019**, *141* (17), 7194–7201.
- (33) Wang, H.; Jung, H.; Song, F.; Zhu, S.; Bai, Z.; Chen, D.; He, G.; Chang, S.; Chen, G. Nitrene-Mediated Intermolecular N–N Coupling for Efficient Synthesis of Hydrazides. *Nat. Chem.* **2021**, *13* (4), 378–385.
- (34) Fan, Q.-K.; Bai, Z.-Q.; He, G.; Chen, G.; Wang, H. Iridium-Catalyzed Nitrene-Mediated Enantioselective 1,2-Hydride Shift Enabled by Attractive Noncovalent Interactions for Chiral δ -Lactam Synthesis. *J. Am. Chem. Soc.* **2025**, *147* (24), 20680–20692.
- (35) Xing, Q.; Chan, C.-M.; Yeung, Y.-W.; Yu, W.-Y. Ruthenium(II)-Catalyzed Enantioselective γ -Lactams Formation by Intramolecular C–H Amidation of 1,4,2-Dioxazol-5-ones. *J. Am. Chem. Soc.* **2019**, *141* (9), 3849–3853.
- (36) Zhou, Z.; Chen, S.; Hong, Y.; Winterling, E.; Tan, Y.; Hemming, M.; Harms, K.; Houk, K. N.; Meggers, E. Non-C2-Symmetric Chiral-at-Ruthenium Catalyst for Highly Efficient Enantioselective Intramolecular C(sp^3)-H Amidation. *J. Am. Chem. Soc.* **2019**, *141* (48), 19048–19057.
- (37) Burg, F.; Rovis, T. Diastereoselective Three-Component 3,4-Amino Oxygenation of 1,3-Dienes Catalyzed by a Cationic Heptamethylinenyl Rhodium(III) Complex. *J. Am. Chem. Soc.* **2021**, *143* (43), 17964–17969.
- (38) Burg, F.; Rovis, T. Rh(III)-Catalyzed Intra- and Intermolecular 3,4-Difunctionalization of 1,3-Dienes via Rh(III)- π -Allyl Amidation with 1,4,2-Dioxazolones. *ACS Catal.* **2022**, *12* (15), 9690–9697.
- (39) Wagner-Carlberg, N.; Rovis, T. Rhodium(III)-Catalyzed Anti-Markovnikov Hydroamidation of Unactivated Alkenes Using Dioxazolones as Amidating Reagents. *J. Am. Chem. Soc.* **2022**, *144* (49), 22426–22432.

- (40) Chen, W.; Xu, H.; Liu, F.-X.; Chen, K.; Zhou, Z.; Yi, W. Chiral Osmium(II)/Salox Species Enabled Enantioselective γ -C(sp³)-H Amidation: Integrated Experimental and Computational Validation For the Ligand Design and Reaction Development. *Angew. Chem., Int. Ed.* **2024**, 63 (20), No. e202401498.
- (41) Fukagawa, S.; Kato, Y.; Tanaka, R.; Kojima, M.; Yoshino, T.; Matsunaga, S. Enantioselective C(sp³)-H Amidation of Thioamides Catalyzed by a Cobalt(III)/Chiral Carboxylic Acid Hybrid System. *Angew. Chem., Int. Ed.* **2019**, 58 (4), 1153–1157.
- (42) Farr, C. M. B.; Kazerouni, A. M.; Park, B.; Poff, C. D.; Won, J.; Sharp, K. R.; Baik, M.-H.; Blakey, S. B. Designing a Planar Chiral Rhodium Indenyl Catalyst for Regio- and Enantioselective Allylic C-H Amidation. *J. Am. Chem. Soc.* **2020**, 142 (32), 13996–14004.
- (43) Mi, R.; Yao, X.; Xu, Y.; Hu, S.; Huang, G.; Li, X. Asymmetric Vicinal and Remote Hydroamination of Olefins by Employing a Heck-Reaction-Derived Hydride Source. *J. Am. Chem. Soc.* **2025**, 147 (20), 17217–17227.
- (44) Song, H.; Mi, R.; Li, X. Rhodium- and Iridium-Catalyzed (Enantioselective) Fluoroamidation of *gem*-Difluoroalkenes via Chelation Assistance. *ACS Catal.* **2025**, 15 (8), 6555–6562.
- (45) Wu, M.; Xu, Y.; Bai, S.; An, Q.; Song, J.; Gao, P.; Li, J.; Huo, J.; Qi, X.; Yan, J.; Xie, W. Cp*Ir(III)-Catalyzed Asymmetric Tandem Intramolecular Aziridination/Aza-Semipinacol Rearrangement of Alkenyl 1,4,2-Dioxazol-5-one. *ACS Catal.* **2025**, 15, 10310–10319.
- (46) Qi, L.-W.; Rogge, T.; Houk, K. N.; Lu, Y. Iridium Nitrenoid-Enabled Arene C-H Functionalization. *Nat. Catal.* **2024**, 7 (8), 934–943.
- (47) Wei, S.-Q.; Li, Z.-H.; Wang, S.-H.; Chen, H.; Wang, X.-Y.; Gu, Y.-Z.; Zhang, Y.; Wang, H.; Ding, T.-M.; Zhang, S.-Y.; Tu, Y.-Q. Asymmetric Intramolecular Amination Catalyzed with Cp*Ir-SPDO via Nitrene Transfer for Synthesis of Spiro-Quaternary Indolinone. *J. Am. Chem. Soc.* **2024**, 146 (28), 18841–18847.
- (48) Wang, H.-H.; Shao, H.; Huang, G.; Fan, J.; To, W.-P.; Dang, L.; Liu, Y.; Che, C.-M. Chiral Iron Porphyrins Catalyze Enantioselective Intramolecular C(sp³)-H Bond Amination Upon Visible-Light Irradiation. *Angew. Chem., Int. Ed.* **2023**, 62 (19), No. e202218577.
- (49) Jin, L.-M.; Xu, P.; Xie, J.; Zhang, X. P. Enantioselective Intermolecular Radical C-H Amination. *J. Am. Chem. Soc.* **2020**, 142 (49), 20828–20836.
- (50) Jin, L.-M.; Xu, X.; Lu, H.; Cui, X.; Wojtas, L.; Zhang, X. P. Effective Synthesis of Chiral *N*-Fluoroaryl Aziridines through Enantioselective Aziridination of Alkenes with Fluoroaryl Azides. *Angew. Chem., Int. Ed.* **2013**, 52 (20), 5309–5313.
- (51) Mas-Roselló, J.; Herraiz, A. G.; Audic, B.; Laverny, A.; Cramer, N. Chiral Cyclopentadienyl Ligands: Design, Syntheses, and Applications in Asymmetric Catalysis. *Angew. Chem., Int. Ed.* **2021**, 60 (24), 13198–13224.
- (52) Laws, D.; Poff, C. D.; Heyboer, E. M.; Blakey, S. B. Synthesis, Stereochemical Assignment, and Enantioselective Catalytic Activity of Late Transition Metal Planar Chiral Complexes. *Chem. Soc. Rev.* **2023**, 52 (17), 6003–6030.
- (53) Hong, S. Y.; Son, J.; Kim, D.; Chang, S. Ir(III)-Catalyzed Stereoselective Haloamidation of Alkynes Enabled by Ligand Participation. *J. Am. Chem. Soc.* **2018**, 140 (39), 12359–12363.
- (54) Hwang, Y.; Park, Y.; Kim, Y. B.; Kim, D.; Chang, S. Revisiting Arene C(sp²)-H Amidation by Intramolecular Transfer of Iridium Nitrenoids: Evidence for a Spirocyclization Pathway. *Angew. Chem., Int. Ed.* **2018**, 57 (41), 13565–13569.
- (55) Hong, S. Y.; Chang, S. Stereodefined Access to Lactams via Olefin Difunctionalization: Iridium Nitrenoids as a Motif of LUMO-Controlled Dipoles. *J. Am. Chem. Soc.* **2019**, 141 (26), 10399–10408.
- (56) Jung, H.; Schrader, M.; Kim, D.; Baik, M.-H.; Park, Y.; Chang, S. Harnessing Secondary Coordination Sphere Interactions That Enable the Selective Amidation of Benzylic C-H Bonds. *J. Am. Chem. Soc.* **2019**, 141 (38), 15356–15366.
- (57) Lee, J.; Lee, J.; Jung, H.; Kim, D.; Park, J.; Chang, S. Versatile Cp*Co(III)(LX) Catalyst System for Selective Intramolecular C-H Amidation Reactions. *J. Am. Chem. Soc.* **2020**, 142 (28), 12324–12332.
- (58) Hong, S. Y.; Kim, D.; Chang, S. Catalytic Access to Carbocation Intermediates via Nitrenoid Transfer Leading to Allylic Lactams. *Nat. Catal.* **2021**, 4 (1), 79–88.
- (59) Lee, J.; Jin, S.; Kim, D.; Hong, S. H.; Chang, S. Cobalt-Catalyzed Intermolecular C-H Amidation of Unactivated Alkanes. *J. Am. Chem. Soc.* **2021**, 143 (13), 5191–5200.
- (60) Kim, S.; Kim, D.; Hong, S. Y.; Chang, S. Tuning Orbital Symmetry of Iridium Nitrenoid Enables Catalytic Diastereo- and Enantioselective Alkene Difunctionalizations. *J. Am. Chem. Soc.* **2021**, 143 (10), 3993–4004.
- (61) Lee, E.; Hwang, Y.; Kim, Y. B.; Kim, D.; Chang, S. Enantioselective Access to Spirolactams via Nitrenoid Transfer Enabled by Enhanced Noncovalent Interactions. *J. Am. Chem. Soc.* **2021**, 143 (17), 6363–6369.
- (62) Liang, H.; Morais, G. N.; Chen, G.; Tang, W.; Zhao, J.; Wang, C.; Houk, K. N.; Chen, S.; Ma, J. Half-Sandwich Ru(II) Complexes Featuring Metal-Centered Chirality: Configurational Stabilization by Ligand Design, Preparation via Kinetic Resolution, and Application in Asymmetric Catalysis. *J. Am. Chem. Soc.* **2025**, 147 (8), 6825–6834.
- (63) Chu, Y.-P.; Yue, X.-L.; Liu, D.-H.; Wang, C.; Ma, J. Asymmetric Synthesis of Stereogenic-at-Iridium(III) Complexes through Pd-Catalyzed Kinetic Resolution. *Nat. Commun.* **2025**, 16 (1), 1177.
- (64) Peris, E.; Crabtree, R. H. Key Factors in Pincer Ligand Design. *Chem. Soc. Rev.* **2018**, 47 (6), 1959–1968.
- (65) Coe, B. J.; Glenwright, S. J. Trans-Effects in Octahedral Transition Metal Complexes. *Coord. Chem. Rev.* **2000**, 203 (1), 5–80.
- (66) Xie, K. A.; Bednarova, E.; Joe, C. L.; Lin, C.; Sherwood, T. C.; Simmons, E. M.; Lainhart, B. C.; Rovis, T. Orange Light-Driven C(sp²)-C(sp³) Cross-Coupling via Spin-Forbidden Ir(III) Metal-laphotoredox Catalysis. *J. Am. Chem. Soc.* **2023**, 145 (36), 19925–19931.
- (67) Xie, K. A.; Bednarova, E.; Joe, C. L.; Sherwood, T. C.; Welin, E. R.; Rovis, T. A Unified Method for Oxidative and Reductive Decarboxylative Arylation with Orange Light-Driven Ir/Ni Metal-laphotoredox Catalysis. *J. Am. Chem. Soc.* **2024**, 146 (37), 25780–25787.
- (68) Bednářová, E.; Grotjahn, R.; Lin, C.; Xie, K. A.; Karube, Y.; Owen, J. S.; Joe, C. L.; Lainhart, B. C.; Sherwood, T. C.; Rovis, T. From Structure to Function: Designing Iridium Catalysts with Spin-Forbidden Excitation for Low-Energy Light-Driven Reactions. *J. Am. Chem. Soc.* **2025**, 147 (15), 12511–12522.
- (69) Obara, S.; Itabashi, M.; Okuda, F.; Tamaki, S.; Tanabe, Y.; Ishii, Y.; Nozaki, K.; Haga, M.-a. Highly Phosphorescent Iridium Complexes Containing Both Tridentate Bis(benzimidazolyl)-benzene or -pyridine and Bidentate Phenylpyridine: Synthesis, Photophysical Properties, and Theoretical Study of Ir-Bis(benzimidazolyl)benzene Complex. *Inorg. Chem.* **2006**, 45 (22), 8907–8921.
- (70) Yi, W.; Chen, W.; Xu, H.; Chen, K.; Zhong, X.; Zhou, Z. Os(II)-Catalyzed γ -C(sp³)-H Amidation and *meta*-C(sp²)-H Alkylation by Fine-Tuning the Characteristics of in-situ-Generated C-Os σ Bonds. *Cell Rep. Phys. Sci.* **2023**, 4 (6), 101423.
- (71) Brulatti, P.; Gildea, R. J.; Howard, J. A. K.; Fattori, V.; Cocchi, M.; Williams, J. A. G. Luminescent Iridium(III) Complexes with N⁴C⁴N-Coordinated Terdentate Ligands: Dual Tuning of the Emission Energy and Application to Organic Light-Emitting Devices. *Inorg. Chem.* **2012**, 51 (6), 3813–3826.
- (72) Hurst, M.; Jarvis, B. Perindopril. *Drugs* **2001**, 61 (6), 867–896.
- (73) Arceo, E.; Jurberg, I. D.; Álvarez-Fernández, A.; Melchiorre, P. Photochemical Activity of a Key Donor-Acceptor Complex can Drive Stereoselective Catalytic α -Alkylation of Aldehydes. *Nat. Chem.* **2013**, 5 (9), 750–756.
- (74) Pierce, J. G.; Kasi, D.; Fushimi, M.; Cuzzupe, A.; Wipf, P. Synthesis of Hydroxylated Bicyclic Amino Acids from L-Tyrosine: Octahydro-1H-indole Carboxylates. *J. Org. Chem.* **2008**, 73 (19), 7807–7810.
- (75) Pansare, S. V.; Lingampally, R.; Kirby, R. L. Stereoselective Synthesis of 3-Aryloctahydroindoles and Application in a Formal Synthesis of (–)-Pancracine. *Org. Lett.* **2010**, 12 (3), 556–559.

(76) Basch, C. H.; Brinck, J. A.; Ramos, J. E.; Habay, S. A.; Yap, G. P. A. Synthesis of *cis*-Octahydroindoles via Intramolecular 1,3-Dipolar Cycloaddition of 2-Acyl-5-aminooxazolium Salts. *J. Org. Chem.* **2012**, *77* (22), 10416–10421.

(77) Kalaitzakis, D.; Triantafyllakis, M.; Ioannou, G. I.; Vassilikogiannakis, G. One-Pot Transformation of Simple Furans into Octahydroindole Scaffolds. *Angew. Chem., Int. Ed.* **2017**, *56* (14), 4020–4023.

(78) Viveros-Ceballos, J. L.; Martínez-Toto, E. I.; Eustaquio-Armenta, C.; Cativiela, C.; Ordóñez, M. First and Highly Stereoselective Synthesis of Both Enantiomers of Octahydroindole-2-phosphonic Acid (OicP). *Eur. J. Org. Chem.* **2017**, *2017* (45), 6781–6787.

(79) Marbán-González, A.; Maravilla-Moreno, G.; Vazquez-Chavez, J.; Hernández-Rodríguez, M.; Razo-Hernández, R. S.; Ordóñez, M.; Viveros-Ceballos, J. L. Stereocontrolled Synthesis of Enantiopure *cis*-Fused Octahydroisindolones via Chiral Oxazoloisindolone Lactams. *J. Org. Chem.* **2021**, *86* (23), 16361–16368.

(80) Bao, X.; Wang, Q.; Zhu, J. Palladium-Catalyzed Enantioselective Desymmetrizing Aza-Wacker Reaction: Development and Application to the Total Synthesis of (–)-Mesembrane and (+)-Crinane. *Angew. Chem., Int. Ed.* **2018**, *57* (7), 1995–1999.

(81) He, Y.-P.; Li, Z.-C.; Wang, Z.-Q.; Zheng, W.-Y.; Wu, H. Enamine Acylation Enabled Desymmetrization of Malonic Esters. *J. Am. Chem. Soc.* **2024**, *146* (38), 26387–26396.

(82) Zhang, F.; Sasmal, H. S.; Daniliuc, C. G.; Glorius, F. Ru-NHC-Catalyzed Asymmetric, Complete Hydrogenation of Indoles and Benzofurans: One Catalyst with Dual Function. *J. Am. Chem. Soc.* **2023**, *145* (29), 15695–15701.



CAS BIOFINDER DISCOVERY PLATFORM™

CAS BIOFINDER HELPS YOU FIND YOUR NEXT BREAKTHROUGH FASTER

Navigate pathways, targets, and
diseases with precision

Explore CAS BioFinder

